Inclusive Hadronic Decay Rate of the τ Lepton from Lattice QCD: The $\bar{u}s$ Flavor Channel and the Cabibbo Angle

Constantia Alexandrou,[1,2] Simone Bacchio,[2] Alessandro De Santis,[3] Antonio Evangelista,[3] Jacob Finkenrath,[4] Roberto Frezzotti,[3] Giuseppe Gagliardi,[5] Marco Garofalo,[6] Bartosz Kostrzewa,[7] Vittorio Lubicz,[8] Simone Romiti,[6] Francesco Sanfilippo,[5] Silvano Simula,[5] Nazario Tantalo,[3] Carsten Urbach,[6] and Urs Wenger[9]

(Extended Twisted Mass Collaboration)

[1]*Department of Physics, University of Cyprus, 20537 Nicosia, Cyprus*
[2]*Computation-based Science and Technology Research Center, The Cyprus Institute, 20 Konstantinou Kavafi Street, 2121 Nicosia, Cyprus*
[3]*Dipartimento di Fisica and INFN, Università di Roma Tor Vergata, Via della Ricerca Scientifica 1, I-00133 Roma, Italy*
[4]*Bergische Universitt Wuppertal, Gaustrae 20, 42119 Wuppertal, Germany*
[5]*Istituto Nazionale di Fisica Nucleare, Sezione di Roma Tre, Via della Vasca Navale 84, I-00146 Rome, Italy*
[6]*HISKP (Theory), Rheinische Friedrich-Wilhelms-Universität Bonn, Nussallee 14-16, 53115 Bonn, Germany*
[7]*High Performance Computing and Analytics Lab, Rheinische Friedrich-Wilhelms-Universität Bonn, Friedrich-Hirzebruch-Allee 8, 53115 Bonn, Germany*
[8]*Dipartimento di Matematica e Fisica, Università Roma Tre and INFN, Sezione di Roma Tre, Via della Vasca Navale 84, I-00146 Rome, Italy*
[9]*Institute for Theoretical Physics, Albert Einstein Center for Fundamental Physics, University of Bern, Sidlerstrasse 5, CH-3012 Bern, Switzerland*

(Received 19 March 2024; revised 14 May 2024; accepted 30 May 2024; published 25 June 2024)

We present a lattice determination of the inclusive decay rate of the process $\tau \mapsto X_{us}\nu_\tau$ in which the τ lepton decays into a generic hadronic state X_{us} with $\bar{u}s$ flavor quantum numbers. Our results have been obtained in $n_f = 2 + 1 + 1$ isosymmetric QCD with full nonperturbative accuracy, without any operator product expansion approximation and, except for the presently missing long-distance isospin-breaking corrections, include a solid estimate of all sources of theoretical uncertainties. This has been possible by using the Hansen-Lupo-Tantalo method [M. Hansen *et al.*, Phys. Rev. D **99**, 094508 (2019)] that we have already successfully applied [A. Evangelista *et al.*, Phys. Rev. D **108**, 074513 (2023)] to compute the inclusive decay rate of the process $\tau \mapsto X_{ud}\nu_\tau$ in the $\bar{u}d$ flavor channel. By combining our first-principles theoretical results with the presently available experimental data, we extract the Cabibbo-Kobayashi-Maskawa matrix element $|V_{us}|$, the Cabibbo angle, with a 0.9% accuracy, dominated by the experimental error.

DOI: 10.1103/PhysRevLett.132.261901

Introduction.—The hadronic decays of the τ lepton represent very important probes of both the leptonic and hadronic flavor sectors of the standard model. A particularly interesting test is the one associated with the Cabibbo angle, more precisely, the Cabibbo-Kobayashi-Maskawa (CKM) matrix element $|V_{us}|$, that can be extracted from both exclusive and inclusive hadronic τ decays and then compared with independent determinations coming from hadronic decays. Currently, the most precise determinations of $|V_{us}|$ are obtained from semileptonic kaon decays, $|V_{us}|_{K_{\ell 3}} = 0.2232(6)$, and from the ratio of the leptonic decay rates of kaons and pions, $|V_{us}|_{K/\pi_{\ell 2}} = 0.2254(5)$ [1,2]. The two determinations exhibit a tension at the level of 2.8 standard deviations (SD).

The exclusive decay rate $\Gamma(\tau \mapsto K\nu_\tau)$ can be computed very precisely in QCD. Indeed, by neglecting long-distance QED radiative corrections, the nonperturbative input needed to compute $\Gamma(\tau \mapsto K\nu_\tau)$ is the same needed to compute the decay rate $\Gamma(K \mapsto \ell\bar{\nu}_\ell)$, namely, the leptonic decay constant f_K. By combining the world average of the lattice QCD results for f_K given in Ref. [1] with the average of the presently available experimental measurements of $\Gamma(\tau \mapsto K\nu_\tau)$, Ref. [3] quotes $|V_{us}|_{\tau\text{-excl}} = 0.2219(17)$, a

value that is well compatible (0.7 SD) with $|V_{us}|_{K_{\ell 3}}$ but lower (2 SD) than $|V_{us}|_{K/\pi_{\ell 2}}$.

The *focus of this Letter* are the inclusive decays of the τ in generic hadronic final states X_{us} with $\bar{u}s$ flavor quantum numbers. We provide, for the first time, first-principles lattice results for the normalized decay rate

$$R_{us}^{(\tau)} = \frac{\Gamma(\tau \mapsto X_{us}\nu_\tau)}{\Gamma(\tau \mapsto e\bar{\nu}_e\nu_\tau)}, \tag{1}$$

that we obtained in $n_f = 2+1+1$ isosymmetric QCD with full nonperturbative accuracy, without any operator product expansion (OPE) approximation and that, except for the presently missing long-distance isospin-breaking corrections [the long-distance QED and strong isospin-breaking corrections (that are presently known only for a limited subset of the exclusive hadronic channels contributing to $\tau \mapsto X_{us}\nu_\tau$) have been neglected in all previous calculations of $R_{us}^{(\tau)}$], include a solid estimate of all sources of theoretical uncertainties.

$R_{us}^{(\tau)}$ is an inclusive quantity that depends upon an energy scale (the τ mass m_τ) which is quite higher than $\Lambda_{\rm QCD}$ and has been extensively studied in the phenomenological literature by relying on asymptotic freedom and by using perturbative and/or OPE approximations. The OPE analysis performed in Refs. [4,5], and recently reviewed in Ref. [3], gives $|V_{us}|_{\tau\text{-OPE-1}} = 0.2184(21)$. A different analysis, performed in Refs. [6,7] by determining the higher order terms in the OPE expansion by fits to lattice current-current correlators and by using a partly different experimental input, gives $|V_{us}|_{\tau\text{-OPE-2}} = 0.2219(22)$. While these two results are compatible at the level of 1 SD, in fact, $|V_{us}|_{\tau\text{-OPE-1}}$ is in strong tension (3.2 SD) with $|V_{us}|_{K/\pi_{\ell 2}}$; see Fig. 3.

A direct nonperturbative lattice calculation of $R_{us}^{(\tau)}$ has been deemed impossible for several years because of the problem associated with the extraction of the needed nonperturbative physical input, i.e., the spectral density of two hadronic weak currents, from the corresponding lattice current-current correlators.

The problem has been circumvented in Ref. [8] by targeting the calculation of spectral integrals that can readily be obtained starting from the lattice current-current correlators. While the method avoids OPE assumptions, it requires perturbative inputs to extract $|V_{us}|$ from the dispersion integral of the measured hadronic τ decays that, in fact, do not provide experimental information on the hadronic spectral density for energies larger than m_τ. The considered dispersion relations have been tailored to minimize the impact of these perturbative inputs, and (taking into account the update of Ref. [7]) the result $|V_{us}|_{\tau\text{-latt-disp}} = 0.2240(18)$ has been obtained. The nice agreement of $|V_{us}|_{\tau\text{-latt-disp}}$ with both $|V_{us}|_{K/\pi_{\ell 2}}$ and $|V_{us}|_{\tau\text{-excl}}$ can be traced back to the fact, emphasized in Ref. [9], that the particular dispersion relation used to get $|V_{us}|_{\tau\text{-latt-disp}}$ mostly relies on the exclusive decay $\tau \mapsto K\nu_\tau$ (which instead contributes for less than 25% to $R_{us}^{(\tau)}$).

In Ref. [10], by building on previous ideas [11,12], we have shown that a direct nonperturbative lattice calculation of inclusive hadronic decay rates of the τ is possible by using the Hansen-Lupo-Tantalo (HLT) method of Ref. [13] for the extraction of smeared spectral densities from lattice correlators. In that companion paper, we provided all the theoretical ingredients needed to directly extract $R_{us}^{(\tau)}$ from the current-current lattice correlators and performed the first nonperturbative calculation of $R_{ud}^{(\tau)}$, i.e., the normalized inclusive decay rate in the $\bar{u}d$ flavor channel. By combining our first-principles lattice result $R_{ud}^{(\tau)}/|V_{ud}|^2 = 3.650(28)$ with the world average of the experimental data given in Ref. [3], we obtained $|V_{ud}|_{\tau\text{-latt-incl}} = 0.9752(39)$. Our result for $|V_{ud}|_{\tau\text{-latt-incl}}$ has a 0.4% error and is fully compatible with the more precise result $|V_{ud}|_{0^+} = 0.973\,73(31)$ coming from superallowed nuclear β decays [14].

In this work, we apply the method of Ref. [10] in the $\bar{u}s$ flavor channel and present our first-principles lattice QCD result

$$R_{us}^{(\tau)}/|V_{us}|^2 = 3.407(22). \tag{2}$$

From this, by using the world average of the experimental data given in Ref. [3], we get

$$|V_{us}|_{\tau\text{-latt-incl}} = 0.2189(7)_{\rm th}(18)_{\rm exp}. \tag{3}$$

Our result, being in very good agreement with both $|V_{us}|_{\tau\text{-OPE-1}}$ and $|V_{us}|_{\tau\text{-OPE-2}}$, confirms the previous estimates of $|V_{us}|$ from inclusive hadronic τ decays and, therefore, also confirms the previous observed tension of about 2–3 SD with respect to other determinations.

Methods.—The method for a direct lattice QCD calculation of $R_{us}^{(\tau)}/|V_{us}|^2$ has been introduced and explained in full detail in Ref. [10]. The starting point of the calculation is the following representation of the normalized inclusive decay rate:

$$\frac{m_\tau^3 R_{us}^{(\tau)}}{12\pi S_{\rm EW}|V_{us}|^2} = \lim_{\sigma\mapsto 0}\sum_{I=T,L}\int_0^\infty dE K_I^\sigma\left(\frac{E}{m_\tau}\right)E^2\rho_I(E^2), \tag{4}$$

which we are now going to illustrate. The factor $S_{\rm EW} = 1.0201(3)$ takes into account the short-distance electroweak corrections [15]. The scalar form factors ρ_T and ρ_L are the transverse (T) and longitudinal (L) components of the hadronic spectral density

$$\begin{aligned}\rho_{us}^{\alpha\beta}(q) &= \langle 0|J_{us}^\alpha(0)(2\pi)^4\delta^4(\mathbb{P}-q)J_{us}^\beta(0)^\dagger|0\rangle \\ &= (q^\alpha q^\beta - g^{\alpha\beta}q^2)\rho_T(q^2) + q^\alpha q^\beta \rho_L(q^2),\end{aligned} \tag{5}$$

where $\mathbb{P}$ is the QCD 4-momentum operator and $J^{\alpha}_{us} = \bar{u}\gamma^{\alpha}(1-\gamma^5)s$ is the hadronic weak current. These also appear in the spectral representation of the following current-current Euclidean correlator:

$$C^{\alpha\beta}(t) = \int d^3x T\langle 0|J^{\alpha}_{us}(t,\boldsymbol{x})J^{\beta}_{us}(0)^{\dagger}|0\rangle. \tag{6}$$

Indeed,

$$C_T(t) = \frac{1}{3}\sum_{i=1}^{3} C^{ii}(t) = \int_0^{\infty}\frac{dE}{2\pi}e^{-Et}E^2\rho_T(E^2),$$
$$C_L(t) = C^{00}(t) = \int_0^{\infty}\frac{dE}{2\pi}e^{-Et}E^2\rho_L(E^2). \tag{7}$$

The kernels

$$K^{\sigma}_L(x) = \frac{(1-x^2)^2\Theta_{\sigma}(1-x)}{x},$$
$$K^{\sigma}_T(x) = (1+2x^2)K^{\sigma}_L(x),$$
$$\Theta_{\sigma}(x) = \frac{1}{1+e^{-\frac{1}{\sigma}}}, \qquad \lim_{\sigma\mapsto 0}\Theta_{\sigma}(x) = \theta(x), \tag{8}$$

are proportional to the phase-space factors and to an infinitely differentiable smooth representation of the Heaviside step function $\theta(x)$ introduced in order to be able to apply the HLT method [13]. In the limit in which the smearing parameter σ vanishes, the energy integral of Eq. (4) is restricted to the physical range $E \in [0, m_{\tau}]$.

As explained in full detail in Ref. [10], it is possible to obtain at finite lattice spacing (a) approximate representations of the kernels $K^{\sigma}_I(E/m_{\tau})$:

$$\tilde{K}^{\sigma}_I\left(\frac{E}{m_{\tau}};\boldsymbol{g}_I\right) = \sum_{n=1}^{N} g_I(n)e^{-naE}, \tag{9}$$

in terms of the coefficients $\boldsymbol{g}_I$. The error of this approximation can be made to vanish in the limit of an infinite number of Euclidean lattice times ($N \mapsto \infty$). The HLT method provides at finite N coefficients $\boldsymbol{g}^{\star}_I$ corresponding to optimal representations

$$\frac{m^3_{\tau}R^{(\tau,I)}_{us}(\sigma)}{24\pi^2 S_{\mathrm{EW}}|V_{us}|^2} = \sum_{n=1}^{N} g^{\star}_I(n)C_I(an) \tag{10}$$

of the smeared spectral integrals appearing in Eq. (4) so that, up to statistical and systematic errors,

$$R^{(\tau)}_{us} = \lim_{\sigma\mapsto 0}\sum_{I=T,L} R^{(\tau,I)}_{us}(\sigma). \tag{11}$$

See the Appendix and Ref. [10] for further details.

TABLE I. ETMC gauge ensembles used in this work. We give the values of the lattice spacing a, of the spatial lattice extent L, and of the vector and axial renormalization constants Z_V and Z_A. The temporal extent of the lattice is always $T = 2L$.

ID	L/a	a (fm)	L (fm)	Z_V	Z_A
B64	64	0.079 51(4)	5.09	0.706 377(20)	0.743 00(21)
B96	96	0.079 51(4)	7.63	0.706 427(10)	0.742 78(20)
C80	80	0.068 16(8)	5.45	0.725 405(14)	0.758 14(13)
C112	112	0.068 16(8)	7.63	0.725 421(10)	0.758 28(11)
D96	96	0.056 88(6)	5.46	0.744 110(7)	0.773 67(8)
E112	112	0.048 91(6)	5.48	0.758 231(5)	0.785 42(7)

Materials.—The lattice gauge ensembles used in this work, generated by the Extended Twisted Mass Collaboration (ETMC), are listed in Table I and described in full detail in Ref. [16]. With respect to that analysis, we have included two additional gauge ensembles, the C112 and the E112 (the ensemble with the finest lattice spacing among those so far produced by the ETMC). Moreover, we have computed the small corrections in the lattice bare parameters required to match the isosymmetric QCD world defined by $f_{\pi} = 130.5\,\mathrm{MeV}$, $m_{\pi} = 135.0\,\mathrm{MeV}$, $m_K = 494.6\,\mathrm{MeV}$, and $m_{D_s} = 1967\,\mathrm{MeV}$. This explains the small difference between the lattice spacings and renormalization constants given in Table I and the ones quoted in Ref. [16].

We relied on the same mixed-action setup described in Refs. [16,17] and evaluated, for each of the ensembles in Table I, the current-current correlator in Eq. (6), extending to the $\bar{u}s$ flavor channel the calculation performed in Ref. [10] in the $\bar{u}d$ sector (to which we refer for further technical details). In full analogy with that calculation, we considered two different regularizations of the weak hadronic current J^{α}_{us}, which give rise to the so-called twisted mass ("tm") and Osterwalder-Seiler ("OS") lattice correlators $C^{\alpha\beta}(t)$. The results for $R^{(\tau)}_{us}(\sigma)$ obtained in the two regularizations differ by $O(a^2)$ cutoff effects [18,19] and must coincide in the continuum limit.

Results.—In our calculation, we considered several values of the smearing parameter $\sigma \in [0.01, 0.16]$ and evaluated $R^{(\tau,I)}_{us}(\sigma)$ on all the ensembles of Table I by using the HLT method. The results of the HLT analyses at $\sigma > 0$, including a quantitative study of the finite-size effects, are presented and discussed in the Appendix. Here, below, we discuss the continuum and $\sigma \mapsto 0$ extrapolations from which we obtain our physical result for $R^{(\tau)}_{us}$. Further technical details on the analysis procedure can be found in Ref. [10].

In Fig. 1, we give an example of the continuum extrapolation for $R^{(\tau)}_{ud}(\sigma)$, which we perform separately for each simulated value of σ. To perform the extrapolations, we take advantage of the fact that in the continuum limit the results corresponding to the tm and OS regularizations must coincide and, thus, perform a combined

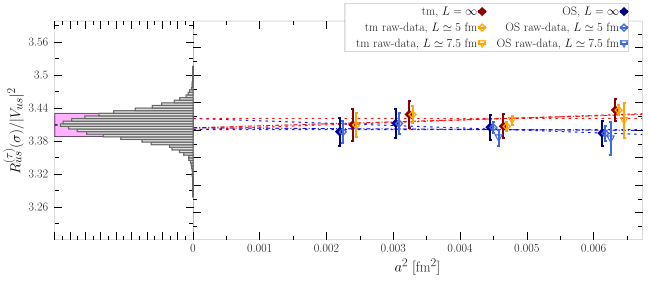

FIG. 1. Illustrative example of the continuum extrapolation of $R^{(\tau)}_{us}(\sigma)$ for $\sigma = 0.02$. The data points in light blue and orange correspond to the raw data obtained on the ensembles listed in Table I, respectively, for the OS and tm regularizations. The data points in dark red and dark blue are instead inclusive of the systematic error due to finite-size effects. The different red (for tm) and blue (for OS) lines show some of the fits obtained using a constant or linear ansatz in a^2. The histogram shown in the left part of the figure corresponds to the distribution of the continuum extrapolated results obtained after applying the BAIC. All data correspond to the kernel reconstructions obtained with the choice $\alpha = r_{\rm max} = 4$ of the HLT algorithmic parameters (see the Appendix).

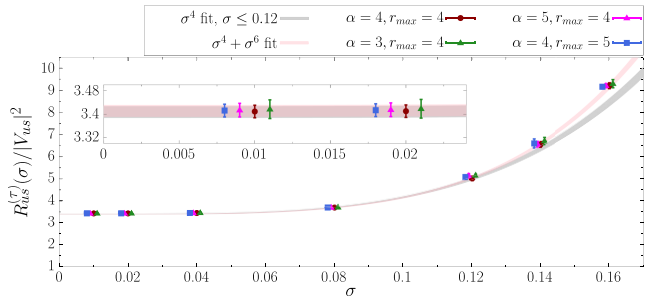

FIG. 2. Extrapolation to vanishing σ. The gray and pink bands correspond, respectively, to the σ^4 and $\sigma^4+\sigma^6$ fits to the data obtained by using $\alpha = r_{\rm max} = 4$ for the HLT algorithmic parameters (see the Appendix). In the case of the σ^4 fit, the data points at $\sigma > 0.12$ have been excluded. The results corresponding to different choices of the HLT algorithmic parameters are in remarkably good agreement.

extrapolation of the form

$$R^{(\tau)}_{us}(\sigma,{\rm tm}) = R(\sigma) + D^{\rm tm}_1(\sigma)a^2 + D^{\rm tm}_2(\sigma)a^4, \qquad (12)$$

$$R^{\tau}_{us}(\sigma,{\rm OS}) = R(\sigma) + D^{\rm OS}_1(\sigma)a^2 + D^{\rm OS}_2(\sigma)a^4, \qquad (13)$$

where $R(\sigma)$, $D^{\rm tm/OS}_1(\sigma)$, and $D^{\rm tm/OS}_2(\sigma)$ are σ-dependent free fit parameters. We perform constant, linear, and quadratic extrapolations in a^2. At small values of $\sigma \lesssim 0.12$, where the size of the cutoff effects is remarkably small, we did not perform fits including the a^4 terms. In order to combine the results obtained in the different correlated continuum fits and provide our final determination of $R^{(\tau)}_{us}(\sigma)$, we make use of the Bayesian Akaike information criterion (BAIC) discussed in Sec. III B in Ref. [10]. The histogram shown in Fig. 1 corresponds to the probability distribution function (p.d.f.) of the continuum extrapolated results. For all σ, we checked that at least one of the fits performed has a χ^2/d.o.f. close to unit. To provide a quantitative measure of the quality of our continuum-limit extrapolations, we considered the spread

$$\Delta_a(\sigma) = \frac{\left|R^{(\tau)}_{us}(\sigma) - R^{(\tau)}_{us}(\sigma, a^{\rm min})\right|}{\Delta R^{(\tau)}_{us}(\sigma)} \qquad (14)$$

between the continuum extrapolated value of $R^{(\tau)}_{us}(\sigma)$ and the corresponding value at the finest simulated lattice spacing (ensemble E112), in units of the uncertainty of the continuum extrapolation $\Delta R^{(\tau)}_{us}(\sigma)$. The lattice spacing dependence is essentially absent within uncertainties for $\sigma < 0.1$, where we have $\Delta_a(\sigma) < 0.1$, while it becomes increasingly pronounced by increasing σ.

To obtain our final determination of $R^{(\tau)}_{us}/|V_{us}|^2$, we need to perform the extrapolation to vanishing σ. According to the theoretical analysis presented in Appendix B in Ref. [10], the corrections to the $\sigma = 0$ limit are of the form

$$R^{(\tau)}_{us}(\sigma) = R^{(\tau)}_{us} + R_4\sigma^4 + \mathcal{O}(\sigma^6). \qquad (15)$$

To carry out the extrapolation and to properly estimate the associated systematic error, we perform a first fit to our data including only σ^4 corrections and considering all values of $\sigma \le 0.12$ and a second, additional, $\sigma^4 + \sigma^6$ fit over the full range of σ explored. The results of these extrapolations are shown in Fig. 2. The $\mathcal{O}(\sigma^6)$ corrections become numerically subleading for $\sigma \le 0.12$, while the σ^4 corrections are subleading for $\sigma \le 0.04$, where the quality of our continuum extrapolations is remarkably good and the dependence upon σ is basically absent. Such behavior allows us to take the $\sigma \mapsto 0$ limit with full confidence.

Figure 2 also shows that the results corresponding to different choices of the HLT algorithmic parameters (see the Appendix) are in perfect agreement, thus confirming the reliability of our estimates of the systematic errors associated with the HLT reconstruction of the smearing kernels.

Taking into account all sources of uncertainties, our final determination of $R^{(\tau)}_{us}/|V_{us}|^2$ is

$$\begin{aligned} R^{(\tau)}_{us}/|V_{us}|^2 &= 3.407(19)_{\rm stat+HLT+FSE}(10)_a(4)_\sigma \\ &= 3.407(22). \end{aligned} \qquad (16)$$

The first source of uncertainty is due to statistical errors and finite-size effects (FSEs) and also includes the systematic uncertainties associated with the HLT spectral reconstructions. (The HLT and FSE systematic errors have been estimated with a data-driven approach [see Eq. (A7)] and,

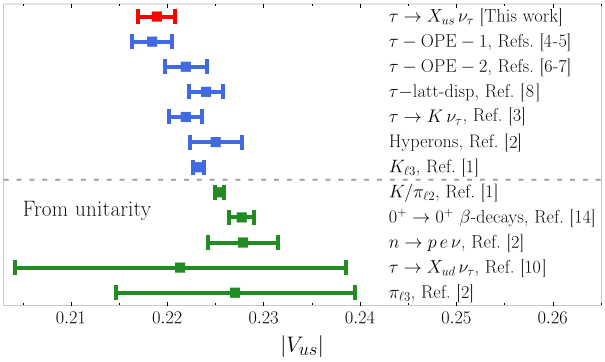

FIG. 3. Comparison between our determination of $|V_{us}|$ (red data point) and existing estimates based on τ-decay analyses or from other decay channels. The lower part of the figure shows the predictions for $|V_{us}|$ obtained assuming CKM unitarity.

therefore, are entangled with the statistical error. Approximately, the HLT systematic error is negligible with respect to the stat and FSE contributions which are instead of similar size.) The second source of uncertainty is due to the continuum-limit extrapolation and has been estimated by taking into account the spread between the results obtained in the different fits using the BAIC [see Eqs. (46) and (47) in Ref. [10] for details]. The third source of uncertainty is due to the $\sigma \mapsto 0$ extrapolation, and it is given by the difference between the results obtained in the σ^4 and $\sigma^4 + \sigma^6$ fits shown in Fig. 2. By combining our theoretical result with the experimental result $R_{us}^{(\tau)} = 0.1632(27)$ quoted in Ref. [3], we obtain

$$|V_{us}|_{\tau\text{-latt-incl}} = 0.2189(7)_{\text{th}}(18)_{\text{exp}}. \tag{17}$$

In Fig. 3, we compare our determination of $|V_{us}|$ with the other existing direct determinations as well as with various determinations obtained by assuming the unitarity of the CKM matrix, i.e., $|V_{us}| = \sqrt{1 - |V_{ud}|^2}$. As the figure shows, our determination of $|V_{us}|$ from inclusive τ decay is in good agreement with both $|V_{us}|_{\tau\text{-OPE-1}}$ and $|V_{us}|_{\tau\text{-OPE-2}}$, while it is smaller (of about 2 SD) than the determination of Ref. [8] which, however, mostly relies on the experimental value of the exclusive $\tau \to K\nu_\ell$ decay.

Our current estimate of $|V_{us}|$ has been obtained by neglecting long-distance isospin-breaking corrections. These, instead, have been taken into account in the determinations $|V_{us}|_{K/\pi_{\ell 2}}$ and $|V_{us}|_{K_{\ell 3}}$ from leptonic and semileptonic decays [20–29]. The current difference between our result in Eq. (17) and the determinations of $|V_{us}|$ from leptonic and semileptonic decays is at the level of 3.3 and 2.2 SD, respectively. We note that in order to fully reconcile the 3.3 SD difference with respect to $|V_{us}|_{K/\pi_{\ell 2}}$ one needs an isospin-breaking correction

$$\delta R_{us}^{(\tau)} = 2\left\{\frac{|V_{us}|_{\tau\text{-latt-incl}}}{|V_{us}|_{K/\pi_{\ell 2}}} - 1\right\} = -0.058(18) \tag{18}$$

on $R_{us}^{(\tau)}$. At the current level of the theoretical precision, a first-principles calculation of $\delta R_{us}^{(\tau)}$ on the lattice is needed. Once this calculation is performed, experimental uncertainties will wholly govern the determination of $|V_{us}|$ from inclusive τ decays.

Conclusions.—In this work, we have extracted for the first time $|V_{us}|$ from inclusive hadronic τ decays with full nonperturbative accuracy and with a 0.9% relative error that, currently, is dominated by the experimental uncertainty.

Our isosymmetric QCD result has been obtained without any perturbative approximation but is in fairly good agreement with previous estimates obtained by using OPE techniques. Therefore, our result confirms the previously observed tension of about 3 SD between τ-inclusive and purely hadronic determinations of $|V_{us}|$ which can no longer be attributed to the OPE approximation.

The origin of this tension can possibly be ascribed to the long-distance isospin-breaking corrections, that have been taken into account in the determinations of $|V_{us}|$ coming from kaons and pions leptonic decays but that, as in all previous determinations coming from inclusive hadronic τ decays, we have presently neglected. In fact, having obtained a fully nonperturbative result with subpercent accuracy in isosymmetric QCD, further progress on the study of inclusive hadronic τ decays can be done only by computing these corrections from first principles. We have already started a series of projects dedicated to this challenging task.

On the other hand, we also noticed that in order to fully reabsorb the observed tension a rather large (of the order of 5%) isospin-breaking correction would be needed. In light of this observation, we think that it is important to investigate the possibility that experimental uncertainties on the τ-inclusive hadronic decay rate have been underestimated and, at the same time, to speculate about possible new physics scenarios that could explain this puzzle.

The authors gratefully acknowledge the Gauss Centre for Supercomputing e.V. for funding this project by providing computing time on the GCS Supercomputers SuperMUC-NG at Leibniz Supercomputing Centre and JUWELS [30] at Juelich Supercomputing Centre. The authors acknowledge the Texas Advanced Computing Center (TACC) at The University of Texas at Austin for providing HPC resources (Project ID No. PHY21001). The authors gratefully acknowledge PRACE for awarding access to HAWK at HLRS within the project with Id Acid 4886. We gratefully acknowledge the Swiss National Supercomputing Centre (CSCS) and the EuroHPC Joint Undertaking for awarding this project access to the

LUMI supercomputer, owned by the EuroHPC Joint Undertaking, hosted by CSC (Finland) and the LUMI consortium through the Chronos program under Project IDs No. CH17-CSCS-CYP and No. CH21-CSCS-UNIBE as well as the EuroHPC Regular Access Mode under Project ID No. EHPC-REG-2021R0095. We gratefully acknowledge CINECA and EuroHPC JU for awarding this project access to Leonardo supercomputing hosted at CINECA. We gratefully acknowledge CINECA for the provision of GPU time under the specific initiative INFN-LQCD123 and IscrB_S-EPIC. V. L., F. S., R. F., and N. T. are supported by the Italian Ministry of University and Research (MUR) under Grant No. PNRR-M4C2-I1.1-PRIN 2022-PE2 Non-perturbative aspects of fundamental interactions, in the Standard Model and beyond F53D23001480006 funded by E.U.—NextGenerationEU. S. S. is supported by MUR under Grant No. 2022N4W8WR. F. S., G. G., and S. S. acknowledge MUR for partial support under Grant No. PRIN20172LNEEZ. F. S. and G. G. acknowledge INFN for partial support under GRANT73/CALAT. F. S. is supported by ICSC Centro Nazionale di Ricerca in High Performance Computing, Big Data and Quantum Computing, funded by European Union NextGenerationEU.

Appendix: HLT analysis.—The HLT coefficients are obtained by considering different definitions of the so-called norm functional,

$$A_I^\alpha[\boldsymbol{g}_I] = \int_{E_{\min}}^{E_{\max}} dE e^{\alpha a E} \left| \tilde{K}_I^\sigma\left(\frac{E}{m_\tau};\boldsymbol{g}_I\right) - K_I^\sigma\left(\frac{E}{m_\tau}\right)\right|^2, \quad \text{(A1)}$$

measuring the squared distance $\|\tilde{K}_I^\sigma - K_I^\sigma\|^2$ in functional space with different definitions of the norm, and by balancing the systematic error associated with an imperfect reconstruction of the smearing kernels and the statistical errors on $R_{us}^{(\tau,I)}(\sigma)$. These are proportional to the so-called error functional

$$B_I[\boldsymbol{g}_I] = \sum_{n_1,n_2=1}^{N} g_I(n_1) g_I(n_2) \mathrm{Cov}_I(an_1, an_2), \quad \text{(A2)}$$

where Cov_I is the covariance matrix of the lattice correlator. At fixed values of the algorithmic parameters $\{N, \alpha, \lambda, E_{\min}, E_{\max}\}$, the coefficients are obtained by minimizing a linear combination of the norm and error functionals:

$$\frac{\partial}{\partial g_I(n)} \left(A_I^\alpha[\boldsymbol{g}_I] + \lambda B_I[\boldsymbol{g}_I]\right)_{\boldsymbol{g}_I = \boldsymbol{g}_I^\lambda} = 0. \quad \text{(A3)}$$

Given the coefficients $\boldsymbol{g}_I^\lambda$, the systematic error associated with the approximate reconstruction of the smearing kernel can be quantified by considering

$$d_I[\boldsymbol{g}_I^\lambda] = \sqrt{\frac{A_I^0[\boldsymbol{g}_I^\lambda]}{A_I^0[\boldsymbol{0}]}}. \quad \text{(A4)}$$

The trade-off parameter λ allows one to cope with the fact that the statistical errors tend to diverge in the $d_I[\boldsymbol{g}_I] \mapsto 0$ and $\sigma \mapsto 0$ limits (see Refs. [31–34] for extended discussions on this point). Indeed, the quality of the kernel reconstruction improves ($d_I[\boldsymbol{g}_I^\lambda]$ decreases) by decreasing λ, while the statistical errors decrease (at the price of larger values of $d_I[\boldsymbol{g}_I^\lambda]$) by increasing λ. The optimal balance between statistical and systematic errors is obtained by studying the stability of the physical results, i.e., of $R_{us}^{(\tau,I)}(\sigma)$ in this case, with respect to variations of the algorithmic parameters.

Stability analyses: By relying on the fact that $\rho_{L,T}(E^2) = 0$ for $E < m_K$, we set $E_{\min} = 0.9 m_K$. The size of the exponential basis, N, has always been fixed by the condition that the uncertainty of $C_I(na)$ for $n \leq N$ must be smaller than 10%. The algorithmic parameter $E_{\max}$ has been set to $E_{\max} = r_{\max}/a$ and different choices of $r_{\max}$ have been employed.

In Fig. 4, we show representative examples of our stability analyses. The robustness of this analysis procedure has been quantitatively assessed in Ref. [31], where it has been introduced, and in the works [10,32,33,35–38], where it has been subsequently applied.

On each ensemble and for each regularization, the uncertainty on $R_{us}^{(\tau,I)}(\sigma)$ is estimated by varying the parameters of the HLT algorithm and by checking that the results are stable within the statistical errors. The stability plots can be read from right to left (and can be understood in analogy with the more familiar effective-mass plots from which the masses of stable hadrons are usually extracted). In the rightmost regions, where $d_I[\boldsymbol{g}_I^\lambda]$ is large, the results strongly depend on the choice of the algorithmic parameters (in the analogy, these are the small-time regions in which effective masses are dominated by excited states). The leftmost regions, where $d_I[\boldsymbol{g}_I^\lambda]$ is very small, correspond to excellent reconstructions of the smearing kernels. In these regions (in the analogy, these are the large-time regions in which the signal on the effective masses of nucleons is usually lost), the coefficients $\boldsymbol{g}_I^\lambda$ tend to become huge in magnitude and oscillating in sign. Neither the central values nor the errors of the results can be trusted when this happens. Indeed, any tiny numerical error on the lattice correlators, even rounding, excludes the possibility of getting trustworthy results for the sums corresponding to Eq. (10) in these cases. A reliable prediction can be obtained when the stability plots show a plateau in the middle region (the effective-mass plateau from which the hadron mass is extracted). By fitting the results in the plateau region, when it exists, one can certainly get a reliable estimate of the errors. As done in the already referenced works [10,31–33,35–38], we decided here to follow a slightly different procedure that, in fact, provides more conservative estimates of the errors. The central values and the statistical errors of our results are quoted by selecting a first reference point in the stability

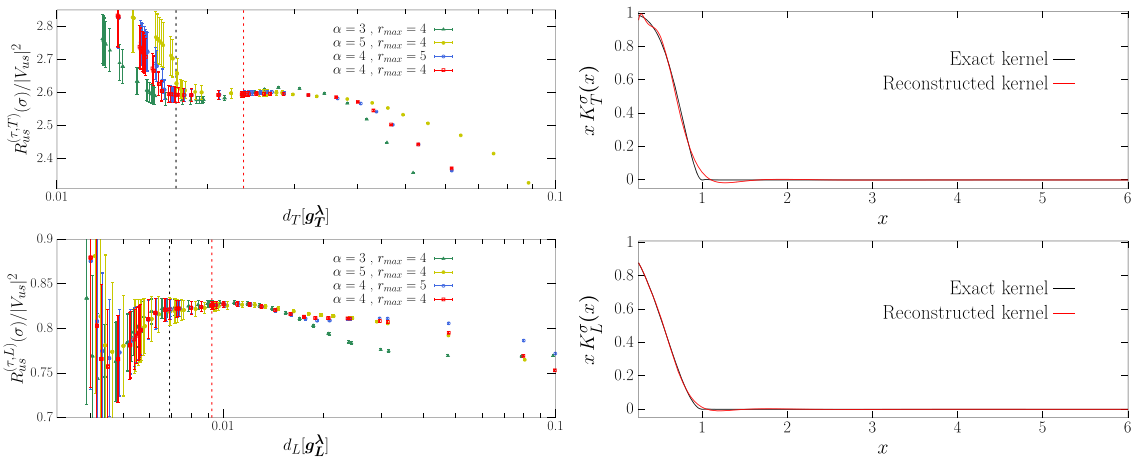

FIG. 4. Left: representative stability-analysis plots for $R_{us}^{(\tau,I)}(\sigma)$. The data are plotted as functions of $d_I[g_I^\lambda]$ [see Eq. (A4)] and refer to the results obtained on the B64 ($R_{us}^{(\tau,T)}$) and D96 ($R_{us}^{(\tau,L)}$) ensembles for $\sigma = 0.02$, using the tm and OS regularization, respectively. In each figure, the points of different colors correspond to different values of the algorithmic parameters α and $r_{\max} = aE_{\max}$, while the red and black vertical lines to the points $d_I[g_I^\star]$ and $d_I[g_I^{\star\star}]$ that we use to extract the central values and errors of our results. Right: comparison between the exact and the reconstructed kernel functions corresponding to the optimal representation obtained in the case $\alpha = r_{\max} = 4$ (red vertical line in the corresponding left plot).

region, corresponding to $g_I^\lambda = g_I^\star$ (red vertical lines in Fig. 4). The choice of $g_I^\star$ is obviously not unique. Any point inside the plateau region can be selected, and the smallest statistical error would be obtained by taking the rightmost one. In this work, we have chosen the $g_I^\star$ points of the different stability analyses in the middle of the plateau regions. The systematic errors associated with the necessarily imperfect reconstruction of the kernels have been estimated by selecting a second reference point on the left of $g_I^\star$, that we call $g_I^{\star\star}$ (black vertical lines in Fig. 4) and that corresponds to the condition

$$\frac{A_I^\alpha[g_I^{\star\star}]}{B_I[g_I^{\star\star}]} = \frac{1}{10}\frac{A_I^\alpha[g_I^\star]}{B_I[g_I^\star]}. \tag{A5}$$

The ratio between the accuracy of the kernel reconstruction and the statistical errors is 10 times smaller at $g_I^{\star\star}$ with respect to $g_I^\star$. The systematic errors have then been quantified by considering the differences

$$dR = R_{us}^{(\tau,I)}(\sigma; g_I^\star) - R_{us}^{(\tau,I)}(\sigma; g_I^{\star\star}) \tag{A6}$$

and their statistical errors (σ_{dR}) and by weighting these differences by the probability that they are not due to statistical fluctuations, i.e.,

$$\Delta_I^{\mathrm{HLT}}(\sigma) = |dR|\mathrm{erf}\left(\frac{dR}{\sqrt{2}\sigma_{dR}}\right). \tag{A7}$$

We performed 672 stability analyses (one for each ensemble, for each lattice regularization, for each value of σ, and for each considered value of α and $r_{\max}$) and found statistical errors typically at the 0.3%–0.5% level of accuracy and systematic errors larger than 3 times the statistical errors in only 2.8% of the cases. The results corresponding to different values of α and $r_{\max}$ have been used to cross check the reliability of our estimates of the HLT systematic errors after having performed, separately, the continuum and $\sigma \mapsto 0$ extrapolations; see Fig. 2 in the main text.

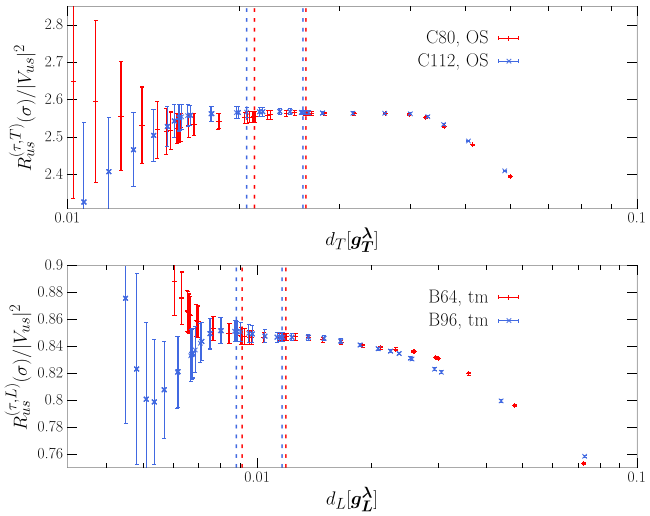

FIG. 5. Top: comparison between the results obtained for $R_{us}^{(\tau,T)}(\sigma)$ on the C80 and C112 ensembles in the OS regularization and for $\sigma = 0.02$. Bottom: comparison between the results obtained for $R_{us}^{\tau,L}(\sigma)$ on the B64 and B96 ensembles in the tm regularization for $\sigma = 0.02$. Data correspond to the reconstruction obtained for $\alpha = r_{\max} = 4$. FSEs are in almost all cases of similar size as the statistical error. In both panels, the vertical lines mark the points $d_I[g_I^\star] > d_I[g_I^{\star\star}]$ for the two ensembles.

Finite-size effects: We carried out a data-driven estimate of the FSEs, which are quantified by the spread between the results obtained on the C80 ($L \sim 5.5$ fm) and on the C112 ($L \sim 7.6$ fm) ensembles, weighted by the probability that this spread is not due to statistical fluctuations and maximized over the tm and OS regularizations [see Eqs. (43) and (44) in Ref. [10]]. We then also checked that these estimates are compatible with the corresponding ones coming from the coarser ensembles B64 and B96 and included the B96 ensemble (not corrected for FSEs) as an extra point in our continuum extrapolations. In Fig. 5, we give examples of such comparison. We have found that FSEs are generally small and of similar size as our statistical accuracy (larger than 2 times the statistical errors in about 1% of the cases).

[1] Y. Aoki *et al.* (Flavour Lattice Averaging Group (FLAG)), FLAG review 2021, Eur. Phys. J. C **82**, 869 (2022).

[2] R. L. Workman *et al.* (Particle Data Group), Review of particle physics, Prog. Theor. Exp. Phys. **2022**, 083C01 (2022).

[3] Y. S. Amhis *et al.* (HFLAV Collaboration), Averages of b-hadron, c-hadron, and τ-lepton properties as of 2021, Phys. Rev. D **107**, 052008 (2023).

[4] E. Gamiz, M. Jamin, A. Pich, J. Prades, and F. Schwab, $|V_{us}|$ and m_s from hadronic tau decays, Nucl. Phys. B, Proc. Suppl. **169**, 85 (2007).

[5] A. Pich, Precision tau physics, Prog. Part. Nucl. Phys. **75**, 41 (2014).

[6] R. J. Hudspith, R. Lewis, K. Maltman, and J. Zanotti, A resolution of the inclusive flavor-breaking $\tau|V_{us}|$ puzzle, Phys. Lett. B **781**, 206 (2018).

[7] K. Maltman *et al.*, Current Status of inclusive hadronic τ determinations of $|V_{us}|$, SciPost Phys. Proc. **1**, 006 (2019).

[8] P. Boyle, R. J. Hudspith, T. Izubuchi, A. Jüttner, C. Lehner, R. Lewis, K. Maltman, H. Ohki, A. Portelli, and M. Spraggs (RBC and UKQCD Collaborations), Novel $|V_{us}|$ determination using inclusive strange τ decay and lattice hadronic vacuum polarization functions, Phys. Rev. Lett. **121**, 202003 (2018).

[9] A. Crivellin, M. Kirk, T. Kitahara, and F. Mescia, Global fit of modified quark couplings to EW gauge bosons and vector-like quarks in light of the Cabibbo angle anomaly, J. High Energy Phys. 03 (2023) 234.

[10] A. Evangelista, R. Frezzotti, N. Tantalo, G. Gagliardi, F. Sanfilippo, S. Simula, and V. Lubicz (Extended Twisted Mass Collaboration), Inclusive hadronic decay rate of the τ lepton from lattice QCD, Phys. Rev. D **108**, 074513 (2023).

[11] M. T. Hansen, H. B. Meyer, and D. Robaina, From deep inelastic scattering to heavy-flavor semileptonic decays: Total rates into multihadron final states from lattice QCD, Phys. Rev. D **96**, 094513 (2017).

[12] P. Gambino and S. Hashimoto, Inclusive semileptonic decays from lattice QCD, Phys. Rev. Lett. **125**, 032001 (2020).

[13] M. Hansen, A. Lupo, and N. Tantalo, Extraction of spectral densities from lattice correlators, Phys. Rev. D **99**, 094508 (2019).

[14] J. C. Hardy and I. S. Towner, Superallowed $0^+ \to 0^+$ nuclear β decays: 2020 critical survey, with implications for V_{ud} and CKM unitarity, Phys. Rev. C **102**, 045501 (2020).

[15] J. Erler, Electroweak radiative corrections to semileptonic tau decays, Rev. Mex. Fis. **50**, 200 (2004).

[16] C. Alexandrou *et al.* (Extended Twisted Mass Collaboration), Lattice calculation of the short and intermediate time-distance hadronic vacuum polarization contributions to the muon magnetic moment using twisted-mass fermions, Phys. Rev. D **107**, 074506 (2023).

[17] R. Frezzotti and G. C. Rossi, Chirally improving Wilson fermions. II. Four-quark operators, J. High Energy Phys. 10 (2004) 070.

[18] R. Frezzotti and G. C. Rossi, Chirally improving Wilson fermions. 1. O(a) improvement, J. High Energy Phys. 08 (2004) 007.

[19] R. Frezzotti, G. Martinelli, M. Papinutto, and G. C. Rossi, Reducing cutoff effects in maximally twisted lattice QCD close to the chiral limit, J. High Energy Phys. 04 (2006) 038.

[20] V. Cirigliano, M. Knecht, H. Neufeld, H. Rupertsberger, and P. Talavera, Radiative corrections to $K_{\ell 3}$ decays, Eur. Phys. J. C **23**, 121 (2002).

[21] V. Cirigliano, M. Giannotti, and H. Neufeld, Electromagnetic effects in $K_{\ell 3}$ decays, J. High Energy Phys. 11 (2008) 006.

[22] V. Cirigliano and H. Neufeld, A note on isospin violation in $P_{\ell 2(\gamma)}$ decays, Phys. Lett. B **700**, 7 (2011).

[23] D. Giusti, V. Lubicz, G. Martinelli, C. T. Sachrajda, F. Sanfilippo, S. Simula, N. Tantalo, and C. Tarantino, First lattice calculation of the QED corrections to leptonic decay rates, Phys. Rev. Lett. **120**, 072001 (2018).

[24] M. Di Carlo, D. Giusti, V. Lubicz, G. Martinelli, C. T. Sachrajda, F. Sanfilippo, S. Simula, and N. Tantalo, Light-meson leptonic decay rates in lattice QCD + QED, Phys. Rev. D **100**, 034514 (2019).

[25] C.-Y. Seng, D. Galviz, M. Gorchtein, and U. G. Meißner, High-precision determination of the K_{e3} radiative corrections, Phys. Lett. B **820**, 136522 (2021).

[26] C.-Y. Seng, D. Galviz, M. Gorchtein, and U.-G. Meißner, Improved K_{e3} radiative corrections sharpen the $K_{\mu 2}$–K_{l3} discrepancy, J. High Energy Phys. 11 (2021) 172.

[27] C.-Y. Seng, D. Galviz, M. Gorchtein, and U.-G. Meißner, Complete theory of radiative corrections to $K_{\ell 3}$ decays and the V_{us} update, J. High Energy Phys. 07 (2022) 071.

[28] P. Boyle *et al.*, Isospin-breaking corrections to light-meson leptonic decays from lattice simulations at physical quark masses, J. High Energy Phys. 02 (2023) 242.

[29] V. Cirigliano, A. Crivellin, M. Hoferichter, and M. Moulson, Scrutinizing CKM unitarity with a new measurement of the $K_{\mu 3}/K_{\mu 2}$ branching fraction, Phys. Lett. B **838**, 137748 (2023).

[30] Jülich Supercomputing Centre, JUWELS cluster and booster: Exascale pathfinder with modular supercomputing architecture at juelich supercomputing centre, J. Large-Scale Res. Facil. **7**, A183 (2021).

[31] J. Bulava, M. T. Hansen, M. W. Hansen, A. Patella, and N. Tantalo, Inclusive rates from smeared spectral densities in the two-dimensional O(3) non-linear σ-model, J. High Energy Phys. 07 (2022) 034.

[32] P. Gambino, S. Hashimoto, S. Mächler, M. Panero, F. Sanfilippo, S. Simula, A. Smecca, and N. Tantalo, Lattice QCD study of inclusive semileptonic decays of heavy mesons, J. High Energy Phys. 07 (2022) 083.

[33] C. Alexandrou *et al.* (Extended Twisted Mass Collaboration (ETMC)), Probing the energy-smeared R ratio using lattice QCD, Phys. Rev. Lett. **130**, 241901 (2023).

[34] M. Buzzicotti, A. De Santis, and N. Tantalo, Teaching to extract spectral densities from lattice correlators to a broad audience of learning-machines, Eur. Phys. J. C **84**, 32 (2024).

[35] A. Barone, S. Hashimoto, A. Jüttner, T. Kaneko, and R. Kellermann, Approaches to inclusive semileptonic $B_{(s)}$-meson decays from Lattice QCD, J. High Energy Phys. 07 (2023) 145.

[36] C. Bonanno, F. D'Angelo, M. D'Elia, L. Maio, and M. Naviglio, Sphaleron rate from a modified Backus-Gilbert inversion method, Phys. Rev. D **108**, 074515 (2023).

[37] R. Frezzotti, N. Tantalo, G. Gagliardi, F. Sanfilippo, S. Simula, and V. Lubicz, Spectral-function determination of complex electroweak amplitudes with lattice QCD, Phys. Rev. D **108**, 074510 (2023).

[38] C. Bonanno, F. D'Angelo, M. D'Elia, L. Maio, and M. Naviglio, Sphaleron rate of $\mathrm{Nf} = 2 + 1$ QCD, Phys. Rev. Lett. **132**, 051903 (2024).